网络出版时间:2025-12-24 16:26:14 网络出版地址:https://link.cnki.net/urlid/34.1065.R.20260115.1419.016

基于miR-34家族靶基因的肺腺癌预后风险评估模型构建与验证

顾铃毓[1],昂格勒玛[2],杨 丹[2],王会峰[3],王利新[1],董 辉[4]

([1]宁夏医科大学总医院心脑血管病医院医学检验科,银川 750000;[2]宁夏医科大学临床医学院,银川 750000;宁夏医科大学总医院[3]肿瘤内科、[4]医学科学研究院,银川 750000)

摘要 **目的** 建立与miR-34家族靶基因相关的肿瘤预后风险评估模型。**方法** 筛选miR-34家族靶基因,检测16例肿瘤中miR-34靶基因的评分。采用单因素Cox回归分析,筛选出miR-34靶基因评分与总生存期(OS)相关性最大的肿瘤。GO和KEGG分析miR-34靶基因的功能和信号通路。通过单因素Cox和LASSO回归分析,构建基于miR-34靶基因的预后风险模型。采用qPCR和双荧光素酶报告基因实验验证其靶基因是否与miR-34结合及在相关肿瘤中的RNA表达水平。此外,将风险评分与其他临床指标相结合,构建用于患者生存的列线图预测模型。**结果** 共筛选到miR-34家族65个靶基因。靶基因评分与OS相关性较强的癌症是肺腺癌(P=0.003,HR=5.150),且miR-34靶基因主要集中在氧化应激途径和多种肿瘤中。*LDHA*、*GALNT7*和*SATB2*三个基因最终被确定为肺腺癌预后分析模型的阵列。**结论** 基于miR-34关键靶基因构建的肺腺癌的风险模型和预后模型具有良好的预测性能。

关键词 miR-34家族靶基因;肺腺癌;总生存期;列线图;预后;风险模型

中图分类号 R 734.2

文献标志码 A **文章编号** 1000-1492(2026)01-0118-09

doi:10.19405/j.cnki.issn1000-1492.2026.01.018

自2002年,Calin et al[1]发现microRNA(miRNA)在慢性淋巴细胞白血病中失调后,miRNA在人类癌症中的作用引起了广泛研究。作为第一个被证明直接受肿瘤抑制基因*p53*调控的miRNA,miR-34家族主要包括miR-34a/34b/34c,当其失调时,可诱导细胞凋亡、细胞衰老及细胞周期阻滞等过程,进而影响肿瘤细胞的发育。研究[2]表明,低水平的循环miR-34或肿瘤特异性miR-34表达与化疗的反应不佳有关。随着第一个基于miR-34a模拟物的肿瘤靶向microRNA药物MRX34在I期临床试验中的应用,miR-34在肿瘤中发挥着愈发重要的作用[3]。因此,课题组在前期对miR-34靶基因进行评分,找出与总生存期(overall survival, OS)相关性较强的癌症之一——肺腺癌(lung adenocarcinoma,LUAD),并建立LUAD预后风险评估模型。

LUAD作为肺癌最常见的病理类型之一,约占

2025-09-20接收

基金项目:宁夏回族自治区重点研发计划项目(编号:2023BEG03033)

作者简介:顾铃毓,女,检验技师;

董 辉,男,副研究员,通信作者,E-mail:173401951@qq.com

digested with collagenase type I and subsequently cultured using an adherent method. Cells were purified *via* differential adhesion and identified through immunofluorescence and Western blotting. ***Results*** CCSMCs began to emerge from the tissue block after 3 days, increased significantly by day 7, and converged by day 12. Post-passage, CCSMCs exhibited strong proliferation and a "peak-to-valley" phenomenon. After purification, the cells tested positive for α-smooth muscle actin (α-SMA), confirming the successful establishment of the *in vitro* culture model. ***Conclusion*** The modified tissue block adherence method is a cost-effective and efficient way to obtain high-purity CCSMCs.

Key words rats; corpus cavernosum smooth muscle cells; smooth muscle actin; vitro model; cell culture; immunofluorescence; tissue block adherence method

Fund programs National Natural Science Foundation of China (Nos. 82474319, 82405412)

Corresponding author Zhang Peihai, E-mail: zhangpeihai@126.com

肺癌的40%[4]。有研究[5]表明，敲除miR-34能够促进小鼠突变 *Kras* 驱动的肺癌进展，且miR-34a/b/c水平较高的肺腺癌患者的生存率高于水平较低的肺腺癌患者。该文分析并建立基于miR-34家族的LUAD预后风险评估模型，以期为LUAD患者潜在生物标志物的筛选及预后判断提供一些参考。

1 材料与方法

1.1 收集癌症数据 从TCGA网站下载包括乳腺癌、结肠癌在内的16种癌症类型的基因表达数据、相关临床数据以及基因体细胞突变数据。包括膀胱尿路上皮癌（bladder urothelial carcinoma，BLCA）、乳腺浸润癌（breast invasive carcinoma，BRCA）、结肠癌（colon adenocarcinoma，COAD）、食管癌（esophageal carcinoma，ESCA）、头颈鳞状细胞癌（head and neck squamous cell carcinoma，HNSC）、肾嫌色细胞癌（kidney chromophobe，KICH）、肾透明细胞癌（kidney renal clear cell carcinoma，KIRC）、肾乳头状细胞癌（kidney renal papillary cell carcinoma，KIRP）、肝细胞肝癌（liver hepatocellular carcinoma，LIHC）、LUAD、肺鳞癌（lung squamous cell carcinoma，LUSC）、前列腺癌（prostate adenocarcinoma，PRAD）、直肠腺癌（rectum adenocarcinoma，READ）、胃癌（stomach adenocarcinoma，STAD）、甲状腺癌（thyroid cancer，THCA）、子宫内膜癌（uterine corpus endometrial carcinoma，UCEC）。同时从UCSC Xena下载相应的生存信息文件。从GEO数据库（https://www.ncbi.nlm.nih.gov/geo/）下载LUAD相关的GSE31210基因表达矩阵及相应的临床数据。

1.2 miR-34靶基因预测及靶基因评分 通过mirDIP、TargetScan和MiRTarBase数据库预测hsa-miR-34a/34b/34c靶向的mRNA，通过交叉3个数据库筛选的miRNA-mRNA对得到miR-34靶基因。根据TCGA中相应的miR-34靶基因表达数据，使用R包GSVA计算16种癌症（包括癌和癌旁样本）中miR-34靶基因的评分，分析算法为ssGSEA。为消除不同癌症类型的数值大小对分析的影响，使结果更方便地显示差异，对原始ssGSEA评分进行Min-Max缩放。

1.3 miR-34靶基因功能富集分析 miR-34靶基因的GO和KEGG富集分析使用R包clusterProfiler，参数设置为default（adj. P<0.05）。

1.4 miR-34靶基因评分差异的肿瘤类型 基于miR-34靶基因评分，采用Wilcoxon检验鉴定各类癌症中的肿瘤组织与癌旁组织之间的差异，并将肿瘤样本与正常样本进行比较，采用多重检验的FDR方法校准P值，最终筛选出miR-34靶基因评分存在差异的肿瘤类型。

1.5 预测并建立模型 从临床资料中提取差异评分癌症患者的生存信息，采用单因素Cox回归分析miR-34靶基因评分与差异评分癌症预后的相关性，以P<0.05为截止标准，筛选与患者生存相关的癌症。通过LASSO-Cox回归分析miR-34靶基因，构建筛查的癌症风险模型。基于构建的Cox比例风险回归模型，计算每位患者的风险评分[6]。根据中位风险评分将患者分为高危组和低危组，并估计两组的Kaplan-Meier生存曲线。计算高危组和低危组的5年生存率，并绘制受试者工作特征（receiver operating characteristic curve，ROC）曲线[7]，以检验模型预测能力的可靠性。对风险模型进行单因素和多因素Cox回归分析，构建列线图。

1.6 双荧光素酶筛选miR-34靶基因 将293T细胞按70%的汇合度接种到96孔板并培养24 h，配制并稀释好DNA和microRNA及转染试剂，常温孵育5 min。将稀释好的DNA和microRNA混匀后再与转染试剂混匀，常温孵育20 min。每孔弃去50 μL培养基，将50 μL DNA -microRNA转染混合液加入孔中。转染6 h后，换新鲜完全培养基。质粒共转染48 h后，弃去培养基，用100 μL PBS洗涤后，吸干剩余的PBS。随后，按双荧光素酶报告基因检测试剂盒操作说明书完成实验。

1.7 荧光定量PCR实验（quantitative real-time PCR，qPCR）检测相关靶基因在LUAD中的表达水平 本研究分析的人LUAD组织微阵列由上海奥特多生物技术有限公司制备，收集并用于PCR检测。用TRIzol试剂从细胞中提取总RNA，用DNase I纯化，用PrimeScript RT试剂反转录成cDNA。采用SYBR®Premix Ex Taq™进行qPCR检测。以β-肌动蛋白为内参数进行荧光定量分析。qPCR反应条件为：95 ℃ 5 min，95 ℃ 10 s，60 ℃ 15 s，72 ℃ 20 s，共40个循环。最后用$2^{-\Delta\Delta C_T}$计算相对表达式。

1.8 统计学处理 采用R 3.3.3进行统计学分析；计数资料用[n(%)]表示；生存分析用Kaplan-Meier法和Log-rank检验；生存相关的独立预后因素分析用单因素和多因素Cox比例风险回归分析；检验水准α=0.05，P<0.05为差异有统计学意义。

表1 引物序列

Tab. 1 Primer sequence

Gene	Primer sequence (5′-3′)
GALNT7	TATCTACCGTCTTGAGGGCTGG
	TGCCTGCGATTCAGGACGACTA
SATB2	CAAGAGTGGCATTCAACCGCAC
	ATCTCGCTCCACTTCTGGCAGA
LDHA	GGATCTCCAACATGGCAGCCTT
	AGACGGCTTTCTCCCTCTTGCT
β-actin	GGCACCCAGCACAATGAA
	TAGAAGCATTTGCGGTGG

2 结果

2.1 miR-34靶基因预测及其在不同癌症中的表达水平 通过mirDIP、TargetScan和MiRTarBase数据库，筛选到92对相交的基因对，去除重复后获得65个miR-34靶基因(图1A)。进一步计算每个miR-34靶基因在所有不同癌症中的表达均值和标准差，然后利用这些均值计算变异系数(coefficient of Variation，CV)，并选择CV值最大的50个基因进行定位。热图显示其在13种具有不同miR-34靶基因评分的癌症中的表达(图1B)。

2.2 miR-34靶基因评分差异对癌症类型的鉴定 基于对16种癌症中65个miR-34靶基因的ssGSEA分析，对16种癌症的所有样本进行miR-34靶基因评分(图2A)。结果显示，16种肿瘤中有3种肿瘤的miR-34靶基因评分在肿瘤与正常之间差异无统计学意义，即HNSC(FDR：0.159)，STAD(FDR：0.052)，THCA(FDR：0.603)。miR-34靶基因评分有显著差异的肿瘤类型包括BLCA、BRCA、COAD、ESCA、KICH、KIRC、KIRP、LIHC、LUAD、LUSC、PRAD、READ和UCEC(图2B)。结合*P*值和风险比，BLCA(*P*=0.007，*HR*=5.870)和LUAD(*P*=0.003，*HR*=5.150)是与OS相关性最强的2种癌症(图2C)。但由于在进一步验证BLCA中miR-34及其相关靶基因是否结合及相关靶基因表达水平时其表现不佳，本文将在后续对LUAD的预后进行分析。

2.3 miR-34靶基因功能及信号通路富集分析 GO分析共产生232个结果，包括220个生物过程(biological process，BP)，12个分子功能(molecular function，MF)，细胞成分(cell component，CC)为0。主要在氧化应激反应、细胞氧化应激反应、过氧化

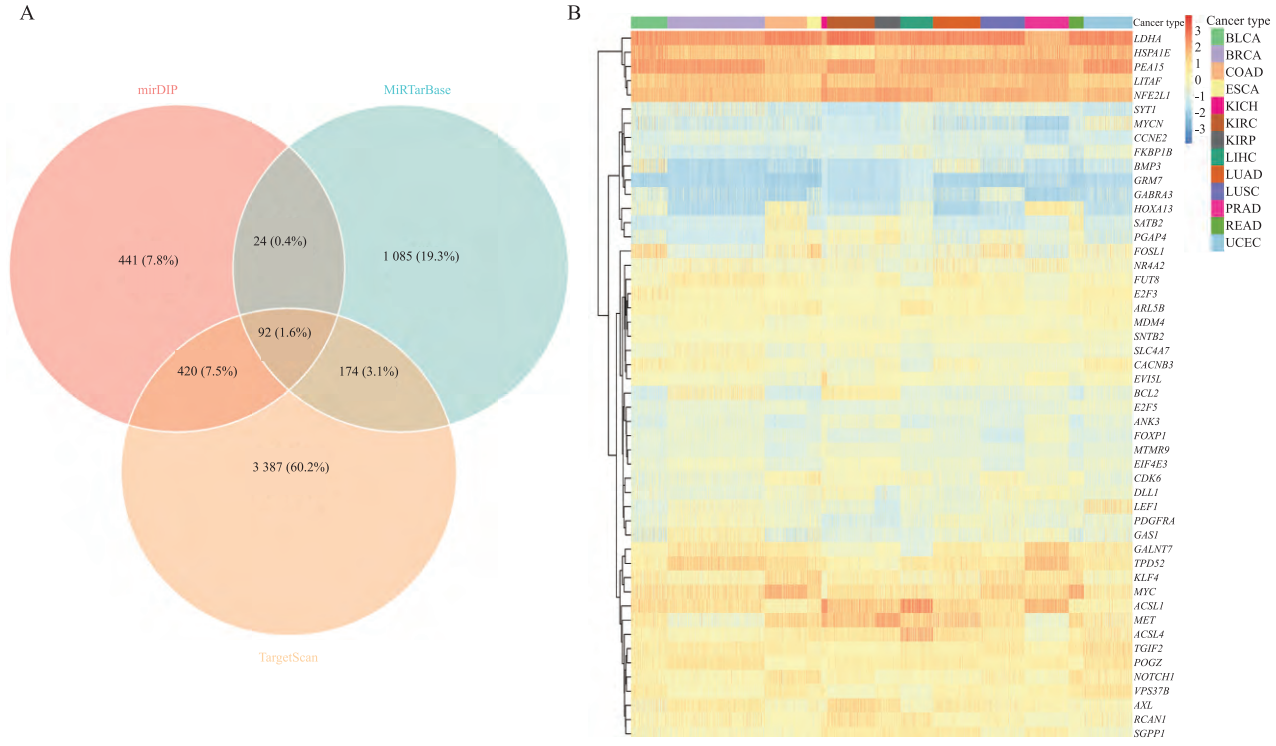

图1 miR-34靶基因预测及其在不同癌症中的表达情况

Fig. 1 Prediction of miR-34 target genes and their expression in different cancers

A: Venn plots of miRNA-mRNA relationship pairs obtained through screening from three databases; B: Heat map of the expression of the top50 target genes with the coefficient of variation among cancer types.

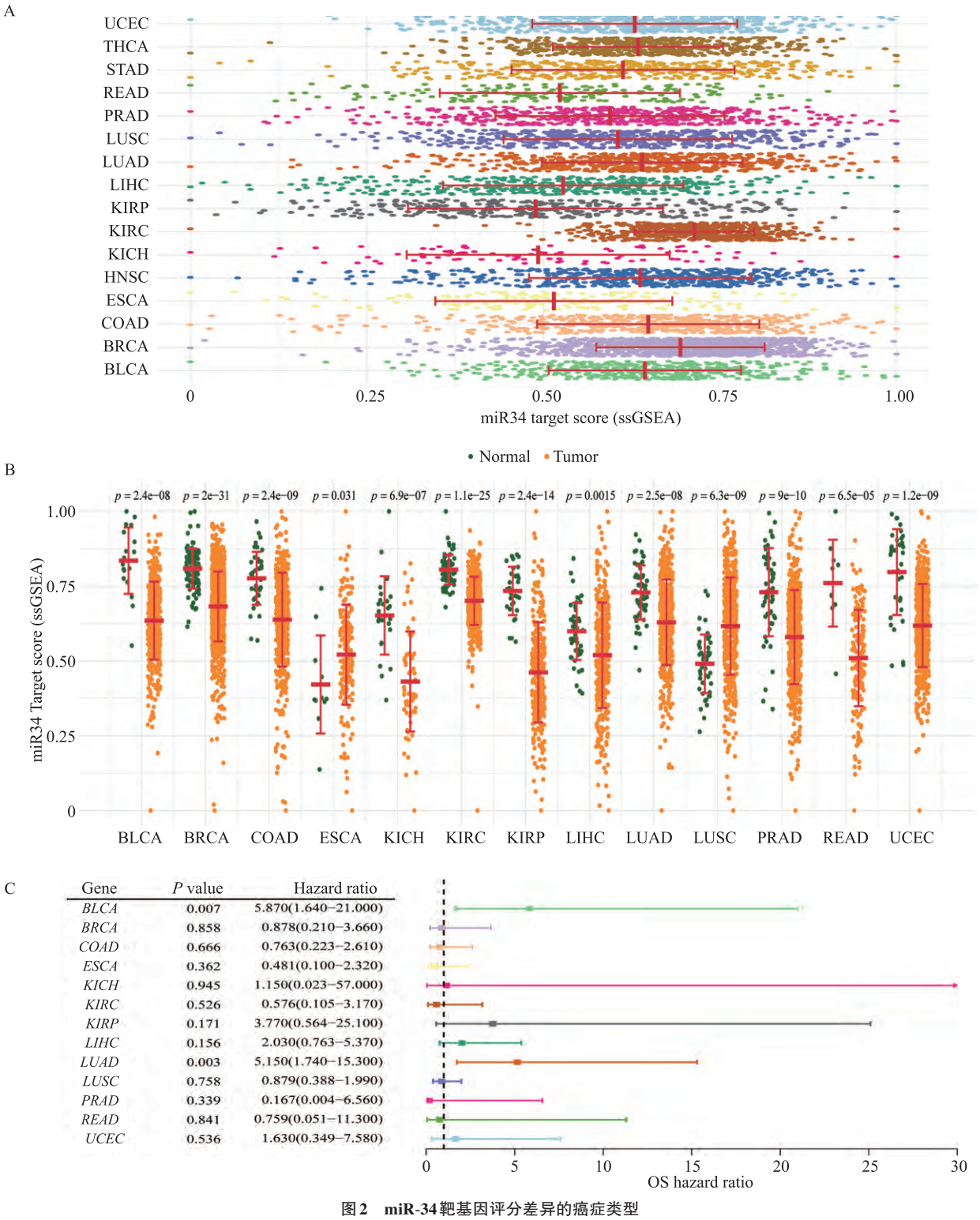

图2 miR-34靶基因评分差异的癌症类型

Fig. 2 Cancer types with differences in miR-34 target gene scores

A: The miR-34 target gene score; The scattered points are the scores of miR-34 target genes; The middle part of the red line segment represents the average; The two ends represent the evaluation distance between the standard deviation and the average; B: Cancer types with significant differences in miR-34 target gene scores; The scattered points are the scores of miR-34 target genes; The middle part of the red line segment represents the average; The two ends represent the evaluation distance between the standard deviation and the average; C: Univariate Cox regression was used to analyze the cancer types most correlated with survival by miR-34 target gene scores.

氢反应等生物功能及RNA聚合酶ii特异性、DNA结合转录因子结合等分子功能方面均发生了显著变化(图3A)。KEGG共输出171条显著变化的小分子核糖核酸通路,例如癌症、细胞衰老、细胞周期、p53信号通路等途径(图3B)。这一结果表明miR-34靶基因主要集中在氧化应激途径和多种肿瘤中。

2.4 LUAD的风险建模 对LUAD中65个miR-34靶基因进行单因素Cox回归分析,结果显示,共有15个基因的表达与OS相关(图4A),将这15个基因用LASSO回归进行分析,并采用最佳模型参数λ=0.026 095 79进行十倍交叉验证筛选。在最优模型下,共有8个基因的系数不为0:*HOXA13*、*GALNT7*、*SATB2*、*SGPP1*、*LDHA*、*KLF4*、*VPS37B*、*FOSL1*。进一步验证这些关键基因是否与miR-34家族存在靶向关系。*GALNT7*、*SATB2*、*LDHA*、*KLF4*、*FOSL*已被验证与miR-34家族具有靶向结合关系。课题组进一步通过双荧光素酶报告基因实验验证*SGPP1*、*HOXA13*和*VPS37B*与miR-34不存在靶向关系(图4B)。因此选择*GALNT7*、*SATB2*、*LDHA*、*KLF4*和*FOSL1* 5个基因进行后续验证。

采用qPCR检测LUAD组织芯片中5个基因的表达情况。结果显示,与癌旁组织相比,*GALNT7*、*SATB2*、*LDHA*在LUAD组织中表达明显升高($P<0.05$),*KLF4*、*FOSL1*在LUAD组织中表达较少(图4C)。继续选择*GALNT7*、*SATB2*和*LDHA* 3个基因作为LUAD预后分析模型的阵列。

采用LASSO回归训练基于*LDHA*、*GALNT7*和*SATB2*的3基因风险模型(图4D)。根据特征系数随λ的变化,确定最优λ为0.002 36(图4E)。采用中位风险评分将患者分为高危组和低危组(图4F)。生存状况显示低危组存活者较多(图4G)。高危组与低危组的生存差异采用相同的log-rank分析,总生存差异有统计学意义($P<0.000\ 1$),低危组患者的生存时间明显长于高危组(图4H)。ROC曲线下的1年、3年和5年生存区分别为0.690、0.668和0.663,说明该模型能够成功预测LUAD患者的预后(图4I)。因此,最终选择了*LDHA*、*GALNT7*和*SATB2*三个基因作为LUAD预后分析模型的阵列。

2.5 LUAD风险模型的外部验证 使用上述训练集得到的风险评分模型在验证集GSE31210中对风险评分进行验证,利用验证集数据计算验证集风险分数,计算公式和训练集一致。根据中位风险评分

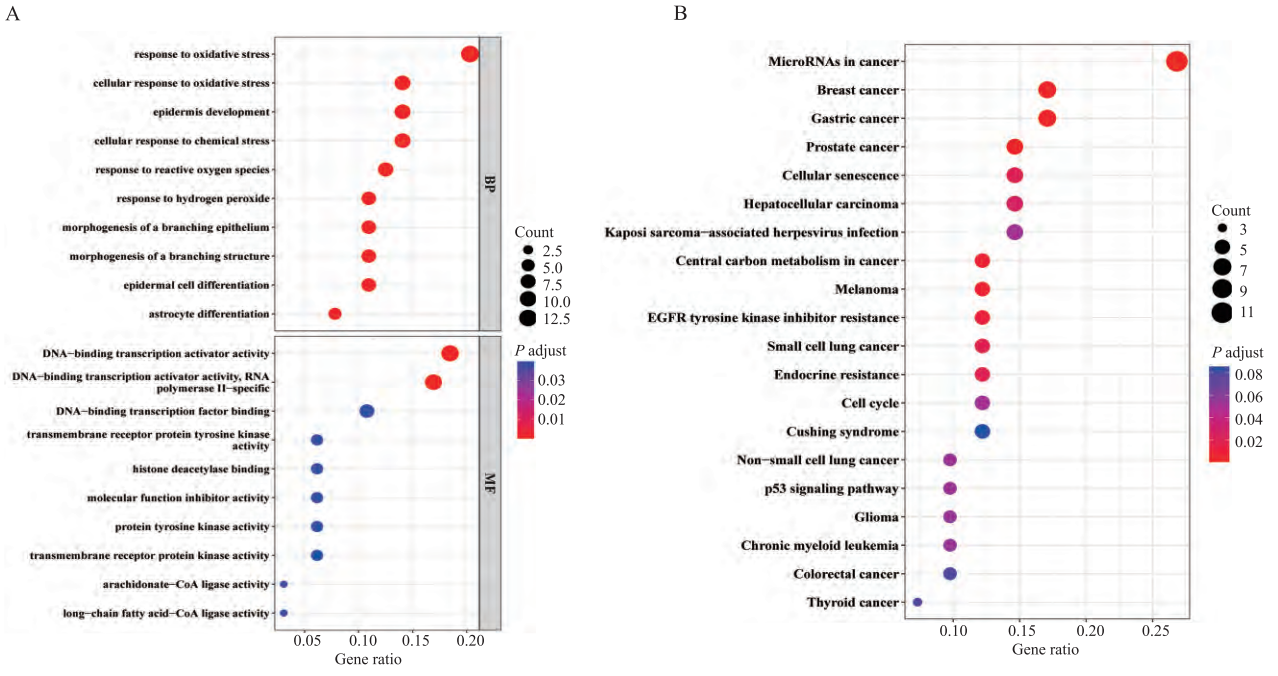

图3 miR-34靶基因的GO和KEGG富集分析

Fig. 3 GO and KEGG enrichment of miR-34 target genes

A: GO function analysis bubble chart; B: KEGG function analysis bubble chart. The horizontal axis represents the ratio, with a larger value indicating a more significant enrichment; The vertical axis is the corresponding name of the enrichment of differentially expressed genes; The size of the bubbles indicates the number of enriched differentially expressed genes; The color of the bubbles ranging from red to blue indicates that the value of *P*. Adjust is getting larger and larger, suggesting that the enrichment is becoming less significant.

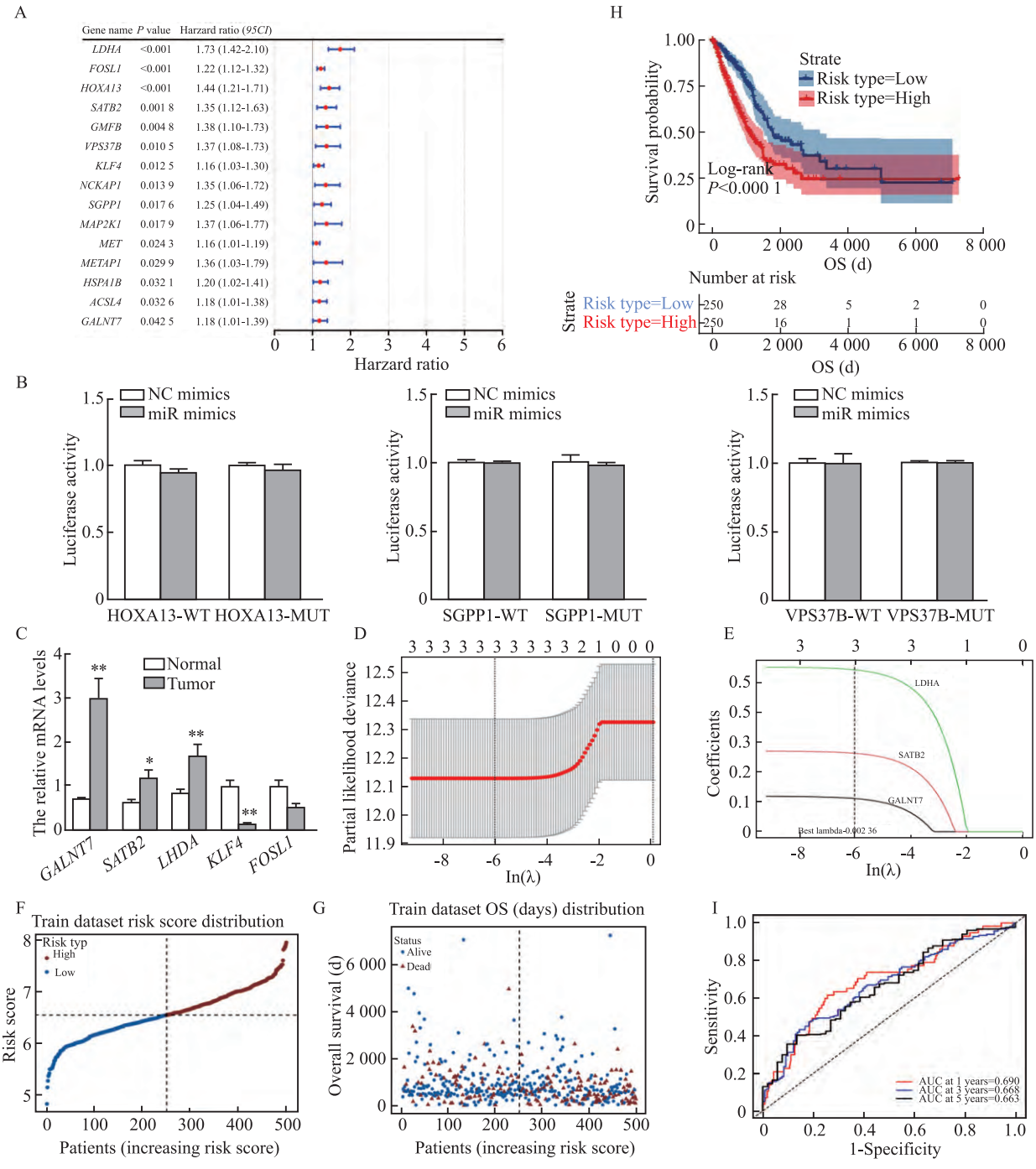

图4 基于miR-34靶基因构建LUAD风险模型

Fig. 4 Construction of the risk model of LUAD by miR-34 target genes

A: Univariate Cox regression model was used to analyze the prognostic genes related to the OS of patients; B: The dual-luciferase reporter gene assay verified the targeted binding relationship of miR-34 with *SGPP1*, *HOXA13* and *VPS37B*; C: The expression of five genes in LUAD tissue microarrays was detected by qPCR; D: The screening process of the cross-validation process parameter λ; E: Dynamic Process Diagram of LASSO-based Variable Screening; F: Distribution of risk scores between high-risk and low-risk patients; G: Distribution of survival status between high-risk and low-risk patients; H: Kaplan-Meier curves for high-risk and low-risk patients; I: ROC curve; $^{*}P<0.05$, $^{**}P<0.01$ *vs* Normal group.

将患者分为高危组和低危组(图5A),生存状况显示低危组存活人数较多(图5B),采用相同的Log-rank分析分析高危组和低危组的生存差异,结果显示低危组和高危组的总生存差异有统计学意义(P=0.028)。低危组患者的生存时间长于高危组(图5C)。1年、3年、5年生存的ROC曲线下面积分别为0.649、0.677、0.681(图5D),表明该模型在验证集中同样适用。

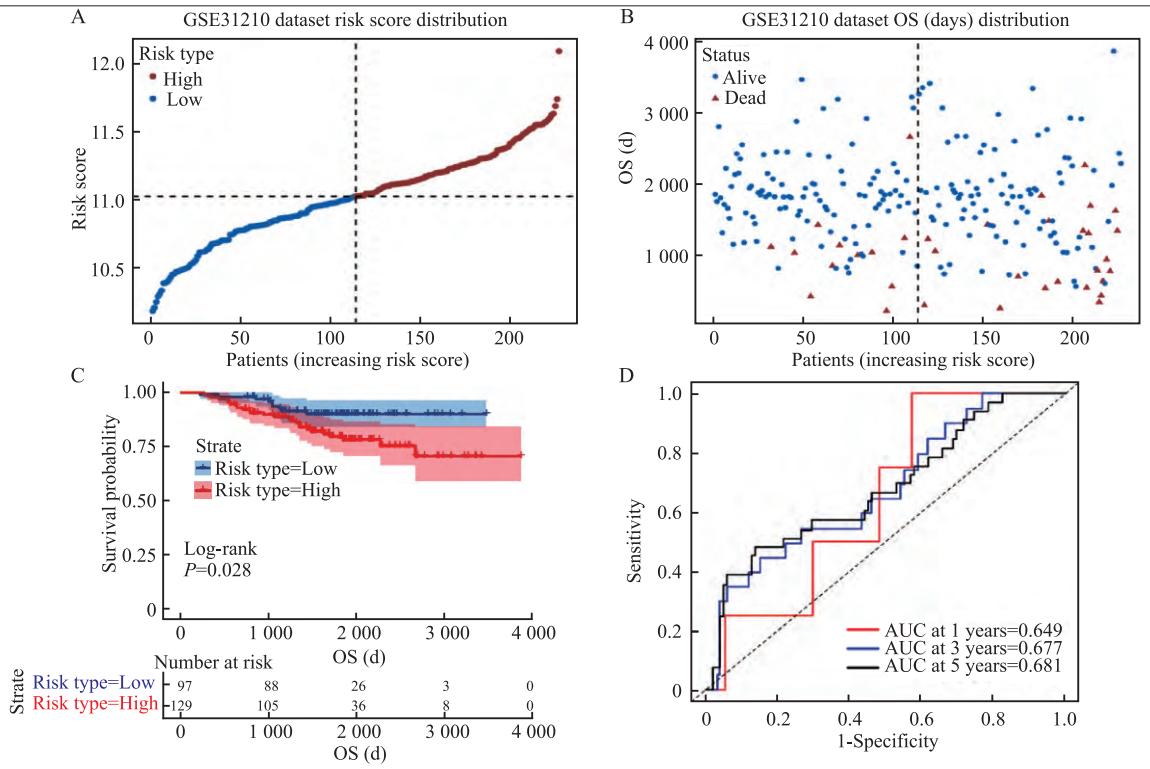

图5 LUAD风险模型验证

Fig. 5 Validation of the LUAD risk model

A: Distribution of risk scores between high-risk and low-risk patients; B: Distribution of risk survival status between high-risk and low-risk patients; C: Kaplan-Meier curves for high-risk and low-risk patients; D: ROC curve.

2.6 基于miR-34靶基因构建LUAD预后模型

将风险评分与其他临床指标相结合，构建预后模型。首先对风险评分、患者年龄、患者性别、肿瘤分期、肿瘤TNM分期7个变量进行单因素Cox回归分析，结果表明肿瘤分期、肿瘤T分期和构建风险评分与患者生存预后相关（$P<0.05$）（图6A、6B）。进一步，利用肿瘤分期、肿瘤T分期和构建的风险评分这3个特征构建多变量Cox模型，并绘制列线图（图6C）。生存预测接近理论直线，表明该模型具有较好的预测性能（图6D）。

3 讨论

在癌症中，miR-34家族基因作为癌基因不断被证明参与肿瘤进展，其中最突出的功能是通过下调多个靶基因抑制肿瘤形成[8]。研究[9]表明，在乳腺癌中，miR-34c主要通过诱导G2/M期阻滞来影响细胞周期。在卵巢癌中，miR-34a/b/c通过触发自噬和凋亡抑制人卵巢癌细胞的增殖，并通过靶向*Notch 1*抑制细胞侵袭。本文通过GO和KEGG分析，验证了miR-34家族靶基因在多种肿瘤中参与多种功能通路和多种信号通路。同时，课题组计算了16种癌症所有样本的miR-34靶基因评分，并使用单变量Cox回归分析，结果显示miR-34靶基因评分与OS相关性较大的癌症是LUAD和BLCA，但由于在进一步验证BLCA中miR-34与其相关靶基因是否结合及相关靶基因表达水平时其表现不佳，最终建立LUAD预后风险评估模型。采用miR-34靶基因评分建立预后模型，在LUAD中筛选*HOXA13*、*GALNT7*、*SATB2*、*SGPP1*、*LDHA*、*KLF4*、*VPS37B*、*FOSL1*等8个基因。参考相关文献[10-13]，筛选掉已验证的靶基因，如*GALNT7*、*SATB2*、*LDHA*、*KLF4*、*FOSL*。课题组后续通过双荧光素酶报告基因实验发现*SGPP1*、*HOXA13*、*VPS37B*与miR-34家族不存在靶向结合。且进一步通过qRT-PCR筛选，选择*GALNT7*、*SATB2*和*LDHA*作为LUAD预后分析模型阵列。

Scott et al[14]通过多个独立的临床队列证明*GALNT7*在前列腺癌组织中上调；研究[15]显示*SATB2*在LUAD组织和A549/CDDP细胞中过表达，且患者预后较差；*LDHA*表达可作为LUAD中不良总生存期和无复发生存期的独立预后指标[2]。因此，将筛选

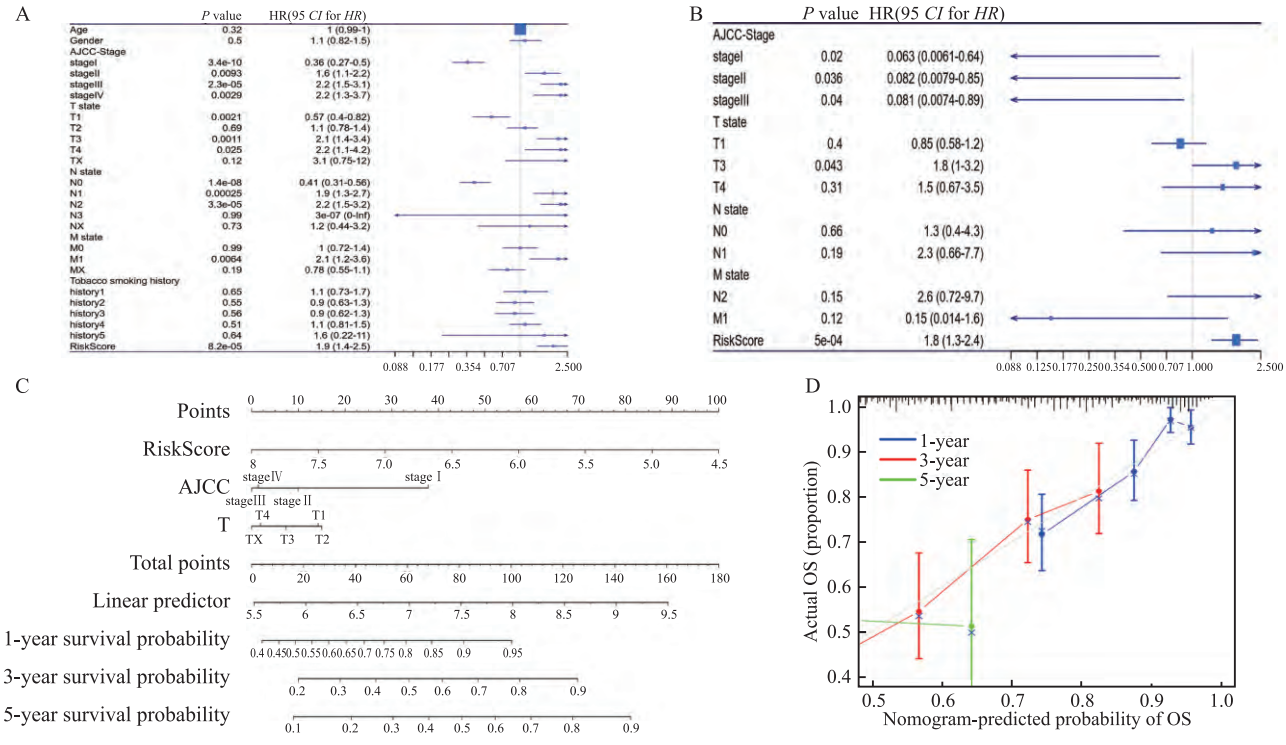

图6 基于miR-34靶基因构建LUAD预后模型

Fig. 6 The prognostic model of LUAD was constructed based on the target genes of miR-34

A: Univariate Cox regression analysis was used to analyze clinical indicators related to prognosis; B: Multivariable Cox model forest map; C: A nomogram constructed using the information of RiskScore, AJCC and T staging; D: Calibration curve of 1-3-5-year survival rate.

到的基因及其系数线性组合作为风险评分,并结合其他临床指标,成功构建了LUAD临床患者生存预测的预后模型。

参考文献

[1] Calin G A, Dumitru C D, Shimizu M, et al. Frequent deletions and down-regulation of micro- RNA genes miR15 and miR16 at 13q14 in chronic lymphocytic leukemia[J]. Proc Natl Acad Sci USA, 2002, 99(24): 15524-9. doi:10.1073/pnas.242606799.

[2] Hwang H W, Mendell J T. microRNAs in cell proliferation, cell death, and tumorigenesis[J]. Br J Cancer, 2006, 94(6): 776-80. doi:10.1038/sj.bjc.6603023.

[3] Agostini M, Knight R A. miR-34: from bench to bedside[J]. Oncotarget, 2014, 5(4): 872-81. doi:10.18632/oncotarget.1825.

[4] 朱亚玉, 凌惠娟, 牛 可, 等. miR-29a介导双氢青蒿素对肺腺癌B7H3分子调控[J]. 安徽医科大学学报, 2025, 60(4): 604-10. doi:10.19405/j.cnki.issn1000-1492.2025.04.003.

[4] Zhu Y Y, Ling H J, Niu K, et al. miR-29a mediates the molecular regulation of dihydroartemisinin on B7H3 in lung adenocarcinoma[J]. Acta Univ Med Anhui, 2025, 60(4): 604-10. doi: 10.19405/j.cnki.issn1000-1492.2025.04.003.

[5] Daugaard I, Knudsen A, Kjeldsen T E, et al. The association between miR-34 dysregulation and distant metastases formation in lung adenocarcinoma[J]. Exp Mol Pathol, 2017, 102(3): 484-91. doi:10.1016/j.yexmp.2017.05.012.

[6] Sui J, Xu S Y, Han J, et al. Integrated analysis of competing endogenous RNA network revealing lncRNAs as potential prognostic biomarkers in human lung squamous cell carcinoma[J]. Oncotarget, 2017, 8(39): 65997-6018. doi: 10.18632/oncotarget.19627.

[7] Heagerty P J, Zheng Y. Survival model predictive accuracy and ROC curves[J]. Biometrics, 2005, 61(1): 92-105. doi: 10.1111/j.0006-341X.2005.030814.x.

[8] Jiang L, Hermeking H. miR-34a and miR-34b/c Suppress Intestinal Tumorigenesis[J]. Cancer Res, 2017, 77(10): 2746-58. doi:10.1158/0008-5472.CAN-16-2183.

[9] Achari C, Winslow S, Ceder Y, et al. Expression of miR-34c induces G2/M cell cycle arrest in breast cancer cells[J]. BMC Cancer, 2014, 14: 538. doi:10.1186/1471-2407-14-538.

[10] Li Y, Zeng C, Hu J, et al. Long non-coding RNA-SNHG7 acts as a target of miR-34a to increase GALNT7 level and regulate PI3K/Akt/mTOR pathway in colorectal cancer progression[J]. J Hematol Oncol, 2018, 11(1): 89. doi: 10.1186/s13045-018-0632-2.

[11] Ge X, Gao J, Sun Q W, et al. miR-34a inhibits the proliferation, migration, and invasion of oral squamous cell carcinoma by directly targeting SATB2[J]. J Cell Physiol, 2020, 235(5): 4856-64. doi:10.1002/jcp.29363.

[12] 李 娜, 李 赟, 万小亚, 等. microRNA-34a调控KLF4转录因子在结直肠癌5-Fu耐药中的作用[J]. 中国肿瘤, 2020, 29(2): 148-53.

[12] Li N, Li Y, Wan X Y, et al. KLF4 transcription factor regulated by microRNA-34a in 5-fu chemotherapy resistance of colorectal cancer[J]. China Cancer, 2020, 29(2): 148-53.
[13] Yang S, Li Y, Gao J, et al. microRNA-34 suppresses breast cancer invasion and metastasis by directly targeting Fra-1[J]. Oncogene, 2013, 32(36): 4294-303. doi:10.1038/onc.2012.432.
[14] Scott E, Hodgson K, Calle B, et al. Upregulation of GALNT7 in prostate cancer modifies O-glycosylation and promotes tumour growth[J]. Oncogene, 2023, 42(12): 926-37. doi: 10.1038/s41388-023-02604-x.
[15] Wang Z, Zhou L, Chen B, et al. microRNA-660 enhances cisplatin sensitivity *via* decreasing SATB2 expression in lung adenocarcinoma [J]. Genes, 2023, 14(4): 911. doi: 10.3390/genes14040911.

Construction and validation of a prognostic risk assessment model for lung adenocarcinoma based on miR-34 family target genes

Gu Lingyu[1], Ang Gelema [2], Yang Dan[2], Wang Huifeng[3], Wang Lixin[1], Dong Hui[4]
([1] *Department of Clinical Laboratory, Cardio-Cerebrovascular Hospital, General Hospital of Ningxia Medical University, Yinchuan* 750000; [2] *Clinical Medical College of Ningxia Medical University, Yinchuan* 750000; [3] *Department of Oncology*, [4] *Institute of Medical Sciences, General Hospital of Ningxia Medical University, Yinchuan* 750000)

Abstract ***Objective*** To establish a tumor prognostic risk assessment model related to target genes of the miR-34 family. ***Methods*** Target genes of the miR-34 family were screened, and the scores of miR-34 target genes were assessed in 16 tumor types. Univariate Cox regression analysis was used to identify the tumor type with the strongest correlation between miR-34 target gene scores and overall survival (OS). Gene Ontology (GO) and Kyoto Encyclopedia of Genes and Genomes (KEGG) analyses were performed to elucidate the functional roles and signaling pathways of miR-34 target genes. A prognostic risk model based on the miR-34 target genes was constructed using univariate Cox and LASSO regression analyses. Quantitative real-time PCR (qPCR) and dual-luciferase reporter assays were conducted to validate whether the target genes bind to miR-34 and measure their RNA expression levels in the relevant tumors. Additionally, the risk score was integrated with other clinical indicators to develop a nomogram prediction model for patient survival. ***Results*** A total of 65 target genes of the miR-34 family were screened. The cancer type exhibiting stronger correlation between the target gene scores and OS was lung adenocarcinoma (P = 0.003, HR= 5.150). Furthermore, miR-34 target genes were predominantly enriched in oxidative stress pathways and various tumor-related processes. Three genes, *LDHA*, *GALNT7*, and *SATB2*, were identified as core components of the prognostic analysis model for lung adenocarcinoma. Additionally, the constructed nomogram model demonstrated robust predictive performance. ***Conclusion*** The risk model and prognosis model of lung adenocarcinoma constructed based on the key target genes of miR-34 have good predictive performance.

Key words miR-34 family target genes; lung adenocarcinoma; overall survival; nomogram; prognosis; risk model
Fund program Key Research and Development Program of Ningxia Hui Autonomous Region (No. 2023BEG03033)
Corresponding author Dong Hui, E-mail: 173401951@qq.com